Physics Letters B 782 (2018) 262–267

Contents lists available at ScienceDirect

Physics Letters B

www.elsevier.com/locate/physletb

Viscous effects on the dynamical evolution of QCD matter during the first-order confinement phase transition in heavy-ion collisions

Bohao Feng [a], Carsten Greiner [b], Shuzhe Shi [c], Zhe Xu [a,*]

[a] Department of Physics, Tsinghua University and Collaborative Innovation Center of Quantum Matter, Beijing, 100084, China
[b] Institut für Theoretische Physik, Johann Wolfgang Goethe-Universität Frankfurt, Max-von-Laue-Strasse 1, 60438, Frankfurt am Main, Germany
[c] Physics Department and Center for Exploration of Energy and Matter, Indiana University, 2401 N Milo B. Sampson Lane, Bloomington, IN 47408, USA

ARTICLE INFO

Article history:
Received 16 February 2018
Received in revised form 7 May 2018
Accepted 10 May 2018
Available online 15 May 2018
Editor: J.-P. Blaizot

ABSTRACT

We investigate viscous effects on the dynamical evolution of QCD matter during the first-order phase transition, which may happen in heavy-ion collisions. We first obtain the first-order phase transition line in the QCD phase diagram under the Gibbs condition by using the MIT bag model and the hadron resonance gas model for the equation of state of partons and hadrons. The viscous pressure, which corresponds to the friction in the energy balance, is then derived from the energy and net baryon number conservation during the phase transition. We find that the viscous pressure relates to the thermodynamic change of the two-phase state and thus affects the timescale of the phase transition. Numerical results are presented for demonstrations.

1. Introduction

A phase diagram separates phases and determines conditions, at which different phases coexist at thermal equilibrium. The completion of the QCD phase diagram [1] is an ongoing task and essential for understanding the matter under strong interaction. Lattice QCD calculations [2] showed that the QCD phase transition at small baryon chemical potential is a crossover rather than a real phase transition. At high baryon chemical potential, theory predicts a first-order phase transition line [3] ending at a QCD critical point [4]. The phase transition of QCD matter can be investigated in experiments of heavy-ion collisions, where quark–gluon plasma (QGP) cools down due to expansion and hadronizes at certain temperature and baryon chemical potential. One major goal of the beam energy scan program at Relativistic Heavy Ion Collider (RHIC) [5–8] is to locate the critical point in the QCD phase diagram.

Usually, a phase transition is defined when two coexisting phases are in thermal equilibrium. The QCD matter produced in heavy-ion collisions possesses, however, a nonzero viscosity [9–11] and deviates from thermal equilibrium. If the system is not far away from thermal equilibrium, one can still define thermodynamic quantities such as temperature, pressure, and chemical potential, as done in viscous hydrodynamic calculations. With these thermodynamic quantities one can also identify the first-order phase transition for the expanding QGP, if the Gibbs condition holds. In this paper we consider nonzero viscosities of QCD matter and investigate viscous effects on the dynamical evolution of QCD matter during the first-order phase transition.

In Sec. 2 we first calculate the first-order phase transition line under the Gibbs condition for phase equilibrium by using MIT bag model and hadron resonance gas model for the equation of state (EoS) of the parton and hadron phase. We then show in Sec. 3 how the shear and bulk viscosity affect the phase transition of the QCD matter produced in heavy-ion collisions. Two different expansion geometries are applied to the evolution of the QCD matter. In Sec. 4 further discussions are given.

2. Phase diagram

Since lattice QCD results of EoS at finite baryon chemical potential are not yet available, we use the EoS from model calculations. Based on these, we present in this section the first-order phase transition line in the temperature–baryon chemical potential diagram.

The parton phase is considered as a system of massless quarks and gluons, which interactions are described by perturbative QCD (pQCD) up to g_s^2 terms [12–14]. The pressure and energy density are

$$P_p = a(T, \mu_q, g_s)T^4 - B\,, \tag{1}$$

* Corresponding author.
E-mail address: xuzhe@mail.tsinghua.edu.cn (Z. Xu).

https://doi.org/10.1016/j.physletb.2018.05.030

$$e_p = 3a(T,\mu_q,g_s)T^4 + B\,, \tag{2}$$

where B is the bag constant with $B^{1/4} = 200$ MeV and

$$a(T,\mu_q,g_s) = \frac{\pi^2}{45}\left[8 + \frac{21}{4}n_f + \frac{45}{2\pi^2}\sum_{i=1}^{n_f}\left(\frac{\mu_i^2}{T^2} + \frac{\mu_i^4}{2\pi^2T^4}\right)\right] - \frac{8}{144}g_s^2\left[3 + \frac{5}{4}n_f + \frac{9}{2\pi^2}\sum_{i=1}^{n_f}\left(\frac{\mu_i^2}{T^2} + \frac{\mu_i^4}{2\pi^2T^4}\right)\right]. \tag{3}$$

μ_i is the chemical potential of a quark flavor. n_f is the number of quark flavors. We consider u, d, s quarks ($n_f = 3$) and assume $\mu_u = \mu_d \equiv \mu_q$, $\mu_{\bar{u}} = \mu_{\bar{d}} = -\mu_q$, and $\mu_s = \mu_{\bar{s}} = 0$. The running coupling is given by [12–14].

$$\alpha_s = \frac{g_s^2}{4\pi} = \frac{12\pi}{33 - 2n_f}\left(\ln\frac{0.8\mu_q^2 + 15.6T^2}{\Lambda_{QCD}^2}\right)^{-1} \tag{4}$$

with $\Lambda_{QCD} = 100$ MeV. From the pressure we obtain the net baryon number density, which is one third of the net quark number density,

$$n_{Bp} = \frac{1}{3}\left.\frac{\partial P_p}{\partial\mu_q}\right|_T \approx \frac{1}{3}n_f\left(1 - \frac{2\alpha_s}{\pi}\right)\left(\mu_q T^2 + \frac{1}{\pi^2}\mu_q^3\right). \tag{5}$$

Here we neglect the logarithmic dependence of α_s on μ_q.

The hadron phase is described by the hadron resonance gas model (HRG) [15–17]. Baryons, mesons, and their resonances having masses up to 2 GeV are included. The pressure and energy density of hadrons and the net baryon number density are given by

$$P_h = \frac{\sum_i P_i^0}{1 + \sum_i n_i^0 v_i} + \frac{\sum_j \bar{P}_j^0}{1 + \sum_j \bar{n}_j^0 v_j} + \sum_m P_m^0\,, \tag{6}$$

$$e_h = \frac{\sum_j e_i^0}{1 + \sum_i n_i^0 v_i} + \frac{\sum_j \bar{e}_j^0}{1 + \sum_j \bar{n}_j^0 v_j} + \sum_m e_m^0\,, \tag{7}$$

$$n_{Bh} = \frac{\sum_i n_i^0}{1 + \sum_i n_i^0 v_i} - \frac{\sum_j \bar{n}_j^0}{1 + \sum_j \bar{n}_j^0 v_j}\,, \tag{8}$$

where i, j, and m denote baryon, antibaryon, and meson, respectively. P_k^0, e_k^0, and n_k^0 are the pressure, energy density, and number density of a hadron species k, when assuming a non-interacting hadron gas,

$$P_k^0(T,\mu_k^h) = \frac{d_k}{6\pi^2}\int dp\frac{p^4}{\sqrt{p^2+m_k^2}}f_k(p)\,, \tag{9}$$

$$e_k^0(T,\mu_k^h) = \frac{d_k}{2\pi^2}\int dp p^2\sqrt{p^2+m_k^2}\,f_k(p)\,, \tag{10}$$

$$n_k^0(T,\mu_k^h) = \frac{d_k}{2\pi^2}\int dp p^2 f_k(p)\,, \tag{11}$$

where d_k is the degeneracy factor and

$$f_k(p) = \left[\exp\left(\frac{\sqrt{p^2+m_k^2} - \mu_k^h}{T}\right) \pm 1\right]^{-1}. \tag{12}$$

$+$ sign is for baryons and $-$ sign is for mesons. m_k denotes the hadron mass and μ_k^h denotes the hadron chemical potential, which relates to the quark chemical potential as $\mu_k^h = \nu_k\mu_q$, where ν_k is the net quark number in hadron k. Thus, $\mu_k^h = 0$ for mesons and $\mu_{\bar{k}}^h = -\mu_k^h$ when $\bar{k}$ denotes the antiparticle of k.

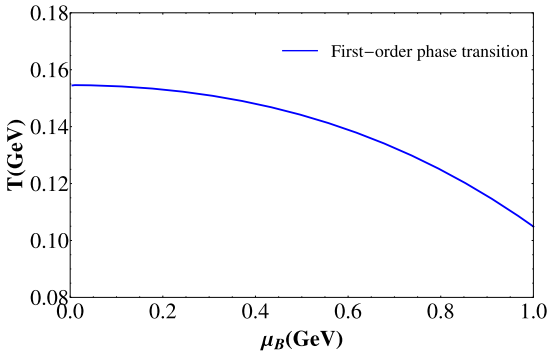

Fig. 1. The QCD first-order phase transition line from model calculations.

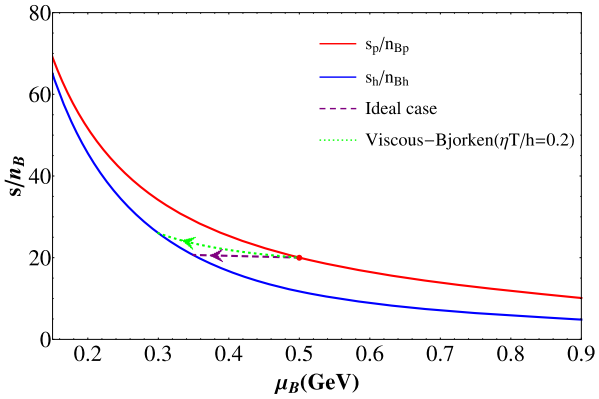

Fig. 2. The ratio s_p/n_{Bp} and s_h/n_{Bh} along the first-order phase transition line. The dashed straight line and dotted curve show the trajectory of s_m/n_{Bm} during the first-order phase transition in an ideal and viscous hydrodynamic expansion, respectively. (For interpretation of the colors in the figure(s), the reader is referred to the web version of this article.)

We take short range repulsive interactions among (anti)baryons into account [15,18–20]. This is indicated in the denominators of the terms in Eqs. (6)–(8), where $v_{i(j)} = 4\pi r_{i(j)}^3/3$ is the eigen volume of baryon i or antibaryon j. We assume a same hard sphere radius for all baryons.

During the first-order phase transition the Gibbs condition holds. The pressure, temperature and baryon chemical potential of both parton and hadron phase are equal. Equating the pressures from Eqs. (1) and (6) with the same temperature T and baryon chemical potential $\mu_B = 3\mu_q$, we obtain the phase boundary curve, which is shown in Fig. 1. The hard-core radius $r_{i(j)}$ of (anti)baryons is set to be 0.6 fm [15]. The calculated curve is similar as those given in [15,21,14].

For the later use the entropy density is given below,

$$s_i = \frac{e_i + P_i - \mu_i n_{Bi}}{T}\,, \tag{13}$$

where the subscript i can be p and h denoting the parton and hadron phase, respectively. We calculate s_p/n_{Bp} and s_h/n_{Bh} along the first-order phase transition line. The results are shown in Fig. 2. We see that s_p/n_{Bp} is larger than s_h/n_{Bh} and both are decreasing with increasing μ_B.

3. Viscous effects during the first-order phase transition

In this section we show how the QCD matter in heavy-ion collisions crosses the first-order phase transition line. For vanishing viscosity the total entropy is conserved. With the conservation of the net baryon number the ratio of the entropy density over the net baryon number density is conserved too. This means that s_h/n_{Bh} at the end of the phase transition should be equal to s_p/n_{Bp} at the beginning of the phase transition. From Fig. 2 we realize that s_p/n_{Bp} is always larger than s_h/n_{Bh} at any given μ_B. Therefore, μ_B (and T) cannot keep constant during the first-order phase transition. Since in addition s_h/n_{Bh} increases with decreasing μ_B, μ_B of the two-phase state will change and move continuously to a smaller value along the first-order phase transition line (see the dashed line in Fig. 2), while T will accordingly move to a larger value [22]. The first-order phase transition will end up at a smaller μ_B (or a larger T). In the following we will study viscous effects on the dynamical evolution of QCD matter during the first-order phase transition. Obviously, μ_B (or T) along the first-order phase transition line will end up at even smaller (larger) value (see the dotted curve in Fig. 2), since more entropy will be produced due to nonzero viscosities.

We consider an expanding system of partons, which is undergoing the first-order confinement phase transition and hadronizing. There should be a clear spatial separation between the parton and hadron phase. Hadron bubbles will be formed. However, the description of the nucleation process is still a challenging issue [23,24]. We can imagine that due to the statistical nature, some of the bubbles are disappearing, while the others are growing and merging until the hadronization is complete. In this article we get around the fluctuating bubble picture in the nucleation process and describe the hadronization on an ensemble average. To this end we assume that each volume element, no matter how small it is, contains separated parton and hadron volumes. Suppose V is the volume of an expanding element in its local rest frame at proper time τ. We denote V_p and V_h as the volume of the parton and hadron phase, respectively. The fraction of the parton phase is then $f_p = V_p/V = V_p/(V_p + V_h)$. The time dependence of f_p describes the hadronization on an ensemble average. The main conclusion of our study that we will present now shows that the effect of nonzero viscosity is to accelerate the decrease of μ_B and to slow down the first-order phase transition.

The energy density and the net baryon number density of the two-phase system in the local rest frame of the considered expanding volume element are

$$e_m = e_p f_p + e_h(1-f_p)\,, \tag{14}$$

$$n_{Bm} = n_{Bp} f_p + n_{Bh}(1-f_p)\,, \tag{15}$$

where e_p, e_h, n_{Bp}, and n_{Bh} are functions of μ_B. (Corresponding T are determined by the first-order phase transition line shown in Fig. 1.) f_p and μ_B are changing with time. Since e_m and n_{Bm} can be solved from the hydrodynamic equations according to the energy and net baryon number conservation, we can determine f_p and μ_B at each time point. The viscosity affects the time evolution of e_m and, thus, affects f_p and μ_B too. The following are the details for determining f_p and μ_B.

Taking time derivative of Eq. (14) gives

$$\frac{\partial e_m}{\partial\tau} = (e_p - e_h)\frac{df_p}{d\tau} + \left[\frac{de_p}{d\mu_B} f_p + \frac{de_h}{d\mu_B}(1-f_p)\right]\frac{\partial\mu_B}{\partial\tau}\,. \tag{16}$$

The left-hand side of the above equation can be obtained from the hydrodynamic equation for the energy density [25,26]

$$De_m = -(e_m + P_c + \Pi_m)\nabla_\mu U^\mu + \pi_m^{\mu\nu}\nabla_{<\mu}U_{\nu>}\,, \tag{17}$$

where U^μ is the fluid four-velocity, $\Pi_m = \Pi_p f_p + \Pi_h(1-f_p)$ is the total bulk pressure, and $\pi_m^{\mu\nu} = \pi_p^{\mu\nu} f_p + \pi_h^{\mu\nu}(1-f_p)$ is the total shear tensor. Since we use the Landau's definition of the fluid four-velocity, there is no heat flow term in Eq. (17). Other symbols in this equation are defined as follows:

$$D \equiv U^\mu\partial_\mu\,, \tag{18}$$

$$\Delta^{\mu\nu} \equiv g^{\mu\nu} - U^\mu U^\nu\,, \tag{19}$$

$$\nabla^\mu \equiv \Delta^{\mu\nu}\partial_\nu\,, \tag{20}$$

$$A^{<\mu\nu>} \equiv \left[\frac{1}{2}\left(\Delta^\mu_\sigma\Delta^\nu_\tau + \Delta^\nu_\sigma\Delta^\mu_\tau\right) - \frac{1}{3}\Delta^{\mu\nu}\Delta_{\sigma\tau}\right]A^{\sigma\tau}\,. \tag{21}$$

We have then

$$\nabla_\mu U^\mu = \partial_\mu U^\mu + \Gamma^\mu_{\alpha\mu}U^\alpha\,, \tag{22}$$

$$\begin{aligned}\nabla^{<\mu}U^{\nu>} = {}& \frac{1}{2}(\partial^\mu U^\nu - U^\mu U^\alpha\partial_\alpha U^\nu + \partial^\nu U^\mu \\ & - U^\nu U^\alpha\partial_\alpha U^\mu) + \frac{1}{2}(\Delta^{\mu\alpha}U^\beta\Gamma^\nu_{\alpha\beta} \\ & + \Delta^{\nu\alpha}U^\beta\Gamma^\mu_{\alpha\beta}) - \frac{1}{3}\nabla_\alpha U^\alpha\Delta^{\mu\nu}\,,\end{aligned} \tag{23}$$

where $\Gamma^\mu_{\alpha\beta} \equiv \frac{1}{2}g^{\mu\nu}(\partial_\beta g_{\alpha\nu} - \partial_\alpha g_{\nu\beta} - \partial_\nu g_{\alpha\beta})$ denotes the Christoffel symbol. By introducing the shear pressure

$$\tilde{\pi}_m = -\frac{\pi_m^{\mu\nu}\nabla_{<\mu}U_{\nu>}}{\nabla_\mu U^\mu}\,, \tag{24}$$

Eq. (17) changes to

$$De_m = -(e_m + P_c + \Pi_m + \tilde{\pi}_m)\nabla_\mu U^\mu\,. \tag{25}$$

In the local rest frame, where $U^\mu = (1,0,0,0)$, we have $De_m = \partial e_m/\partial\tau$ and

$$\nabla_\mu U^\mu = \frac{1}{V}\frac{dV}{d\tau}\,. \tag{26}$$

By equating the right-hand side of both Eqs. (16) and (25) we obtain

$$\begin{aligned}\frac{df_p}{d\tau} = {}& -\frac{e_m + P_c + \Pi_m + \tilde{\pi}_m}{e_p - e_h}\frac{1}{V}\frac{dV}{d\tau} \\ & - \frac{1}{e_p - e_h}\left[\frac{de_p}{d\mu_B}f_p + \frac{de_h}{d\mu_B}(1-f_p)\right]\frac{\partial\mu_B}{\partial\tau}\,.\end{aligned} \tag{27}$$

Analogously to the derivation from Eqs. (14) and (17) to Eq. (27), we can also derive $df_p/d\tau$ from the net baryon number density (15) and its hydrodynamic evolution

$$Dn_{Bm} = -n_{Bm}\nabla_\mu U^\mu\,, \tag{28}$$

which indicates the net baryon number conservation. In the present study we have neglected the diffusion current induced by the heat conduction. We have then

$$\begin{aligned}\frac{df_p}{d\tau} = {}& -\left(\frac{n_{Bh}}{n_{Bp} - n_{Bh}} + f_p\right)\frac{1}{V}\frac{dV}{d\tau} - \frac{1}{n_{Bp} - n_{Bh}} \\ & \times\left[\frac{dn_{Bp}}{d\mu_B}f_p + \frac{dn_{Bh}}{d\mu_B}(1-f_p)\right]\frac{\partial\mu_B}{\partial\tau}\,.\end{aligned} \tag{29}$$

Equating Eq. (27) and Eq. (29) gives

$$\Pi_m + \tilde{\pi}_m = \frac{n_{Bh}(e_p - e_h)}{n_{Bp} - n_{Bh}} - (e_h + P_c) + C_1\frac{1}{\frac{1}{V}\frac{dV}{d\tau}}\frac{\partial\mu_B}{\partial\tau}\,, \tag{30}$$

where

$$C_1 = \left(\frac{e_p - e_h}{n_{Bp} - n_{Bh}}\frac{dn_{Bp}}{d\mu_B} - \frac{de_p}{d\mu_B}\right) f_p + \left(\frac{e_p - e_h}{n_{Bp} - n_{Bh}}\frac{dn_{Bh}}{d\mu_B} - \frac{de_h}{d\mu_B}\right)(1 - f_p)\,. \tag{31}$$

In the first-order theory of hydrodynamics, the bulk pressure and shear stress tensor are proportional to the bulk and shear viscosity [25,27,28],

$$\Pi_m = -\xi_m \nabla_\mu U^\mu\,, \tag{32}$$

$$\pi_m^{\mu\nu} = 2\eta_m \nabla^{<\mu} U^{\nu>}\,. \tag{33}$$

η_m and ξ_m are the shear and bulk viscosity of the two-phase system and $\eta_m = \eta_p f_p + \eta_h(1-f_p)$ and $\xi_m = \xi_p f_p + \xi_h(1-f_p)$, where η_p and η_h (ξ_p and ξ_h) are the shear (bulk) viscosity of the parton and hadron phase respectively. If all the viscosities and the fluid velocity are known, we can solve $\mu_B(\tau)$ from Eq. (30) and then $f_p(\tau)$ from Eq. (27) or Eq. (29).

As stated at the beginning of this section, μ_B should decrease along the first-order phase transition line. However, from Eq. (30) it is not obvious that $\partial\mu_B/\partial\tau$ is negative even for vanishing viscosities. We now look at the entropy of the two-phase system, which is

$$s_m \equiv \frac{e_m + P_c - \mu_B n_{Bm}}{T} = s_p f_p + s_h(1 - f_p) \tag{34}$$

according to Eqs. (14) and (15), and the definition (13). The time evolution of s_m is obtained from the time evolution of e_m and n_{Bm}, namely Eqs. (17) and (28). We have

$$\frac{\partial s_m}{\partial\tau} = -s_m \nabla_\mu U^\mu + \frac{\Pi_m^2}{\xi_m T} + \frac{\pi_{m,\mu\nu}\pi_m^{\mu\nu}}{2\eta_m T} \tag{35}$$

for the first-order viscous hydrodynamics. Analogously to the derivation of Eq. (27) we get

$$\frac{df_p}{d\tau} = -\frac{Ts_m + \Pi_m + \tilde{\pi}_m}{T(s_p - s_h)}\frac{1}{V}\frac{dV}{d\tau} - \frac{1}{s_p - s_h}\left[\frac{ds_p}{d\mu_B} f_p + \frac{ds_h}{d\mu_B}(1 - f_p)\right]\frac{\partial\mu_B}{\partial\tau}\,. \tag{36}$$

Equating Eq. (36) with Eq. (29) gives then

$$\Pi_m + \tilde{\pi}_m = T\left(\frac{s_p}{n_{Bp}} - \frac{s_h}{n_{Bh}}\right)\frac{n_{Bp} n_{Bh}}{n_{Bp} - n_{Bh}} + C_2 \frac{T}{\frac{1}{V}\frac{dV}{d\tau}}\frac{\partial\mu_B}{\partial\tau}\,, \tag{37}$$

where

$$C_2 = \left(\frac{s_p - s_h}{n_{Bp} - n_{Bh}} - \frac{ds_p}{dn_{Bp}}\right)\frac{dn_{Bp}}{d\mu_B} f_p + \left(\frac{s_p - s_h}{n_{Bp} - n_{Bh}} - \frac{ds_h}{dn_{Bh}}\right)\frac{dn_{Bh}}{d\mu_B}(1 - f_p)\,. \tag{38}$$

With the Gibbs–Duhem equation $dP = sdT + nd\mu$ one can prove that Eqs. (30) and (37) are identical. Since both s_p/n_{Bp} and s_h/n_{Bh} decrease with increasing μ_B (see Fig. 2), i.e., $d(s_p/n_{Bp})/d\mu_B < 0$ and $d(s_h/n_{Bh})/d\mu_B < 0$, one obtains easily $ds_p/dn_{Bp} < s_p/n_{Bp}$ and $ds_h/dn_{Bh} < s_h/n_{Bh}$. We have then

$$C_2 > \left(\frac{s_p}{n_{Bp}} - \frac{s_h}{n_{Bh}}\right)\left[\frac{n_{Bh}}{n_{Bp} - n_{Bh}}\frac{dn_{Bp}}{d\mu_B} f_p + \frac{n_{Bp}}{n_{Bp} - n_{Bh}}\frac{dn_{Bh}}{d\mu_B}(1 - f_p)\right] > 0 \tag{39}$$

for $s_p/n_{Bp} > s_h/n_{Bh}$ (see Fig. 2). From Eq. (37) we realize that $\partial\mu_B/\partial\tau$ is always negative and its absolute value becomes larger for increasing viscosity. [Remember that Π_m and $\tilde{\pi}_m$ are negative for the first-order viscous hydrodynamics when the system is expanding and they are proportional to the bulk and shear viscosity according to Eqs. (24), (32), and (33).] The viscous effect leads to a stronger decrease of μ_B during the first-order phase transition, compared to the ideal hydrodynamic expansion. Moreover, according to Eq. (29) the decrease of f_p slows down in the viscous case. The larger the viscosity, the longer will the phase transition take.

For demonstrating the viscous effects we now calculate explicitly the time evolution of μ_B and f_p during the first-order phase transition with given fluid velocity and viscosities. We compare the results with nonzero viscosities to those with zero viscosities.

To this end we use the analytical solutions of U^μ from one-dimensional Bjorken expansion [29] and three-dimensional Gubser expansion [30,31]. Be $U^\mu = \gamma(1, \mathbf{v})$ with $\gamma = 1/\sqrt{1 - v^2}$ in the space time coordinate $(t, \mathbf{r})$. With the time $\tilde{\tau} = \sqrt{t^2 - z^2}$, the space time rapidity $\eta = (1/2)\ln(t+z)/(t-z)$, the transverse radius $\rho = \sqrt{x^2 + y^2}$ and the azimuthal angle ϕ, the fluid velocity can be transformed into the coordinate $(\tilde{\tau}, \eta, \rho, \phi)$ as follows [32]:

$$\begin{aligned} U^{\tilde{\tau}} &= \gamma(\cosh\eta - v_z \sinh\eta)\,,\\ U^{\eta} &= \frac{\gamma}{\tilde{\tau}}(v_z \cosh\eta - \sinh\eta)\,,\\ U^{\rho} &= \gamma(v_x \cos\phi + v_y \sin\phi)\,,\\ U^{\phi} &= \gamma(v_y \cos\phi - v_x \sin\phi)\,. \end{aligned} \tag{40}$$

U^μ in Bjorken expansion is given in the coordinate $(t, \mathbf{r})$ [29],

$$v_x = v_y = 0\,,\ v_z = \frac{z}{t}\,, \tag{41}$$

while U^μ in Gubser expansion is given in the coordinate $(\tilde{\tau}, \eta, \rho, \phi)$ [30,31],

$$U^{\tilde{\tau}} = \cosh k\,,\ U^{\rho} = \sinh k\,,\ U^{\eta} = U^{\phi} = 0\,, \tag{42}$$

where

$$\tanh k = \frac{2\tilde{\tau}\rho}{a^2 + \tilde{\tau}^2 + \rho^2}\,. \tag{43}$$

Different from the Bjorken expansion, the Gubser expansion includes transverse expansion. The parameter a is set to be 4.5 fm. A similar value has been used to describe the hydrodynamic evolution of QGP in Au+Au collisions at RHIC with $\sqrt{s_{NN}} = 200$ GeV [30,33]. In addition we choose $\rho = 0$ in our calculations. The phase transition in volume elements with larger transverse radius ρ will occur earlier. For Bjorken expansion and for Gubser expansion at $\rho = 0$, $\tilde{\tau}$ is equal to the proper time in the local rest frame, τ.

Although there are calculations and model-to-data analyses on the shear and bulk viscosity of the parton and/or hadron phase in heavy-ion collisions [34–41], the shear and bulk viscosity of both phases during the first-order phase transition are not yet fixed so far. We assume *for simplicity* that the shear and bulk viscosity in the parton phase are equal and the shear and bulk viscosity in the hadron phase are twice as much as those in the parton phase. Moreover, we set $\eta_p T/h_p = \xi_p T/h_p$ to be constant during the phase transition. $h_p = e_p + P_c$ is the enthalpy density of partons. At $\mu_B = 0$, h_p/T is equal to the entropy density. $\eta_p T/h_p$ and $\xi_p T/h_p$ are more relevant to characterize the viscous effect in slow expansion [42] as will happen in heavy-ion collisions with lower colliding energies.

In Fig. 3 the time evolution of μ_B and f_p are presented with three different values of viscosities, $\eta_p T/h_p = \xi_p T/h_p = 0, 0.2, 0.4$, and with two different expansion dynamics, Bjorken and Gubser

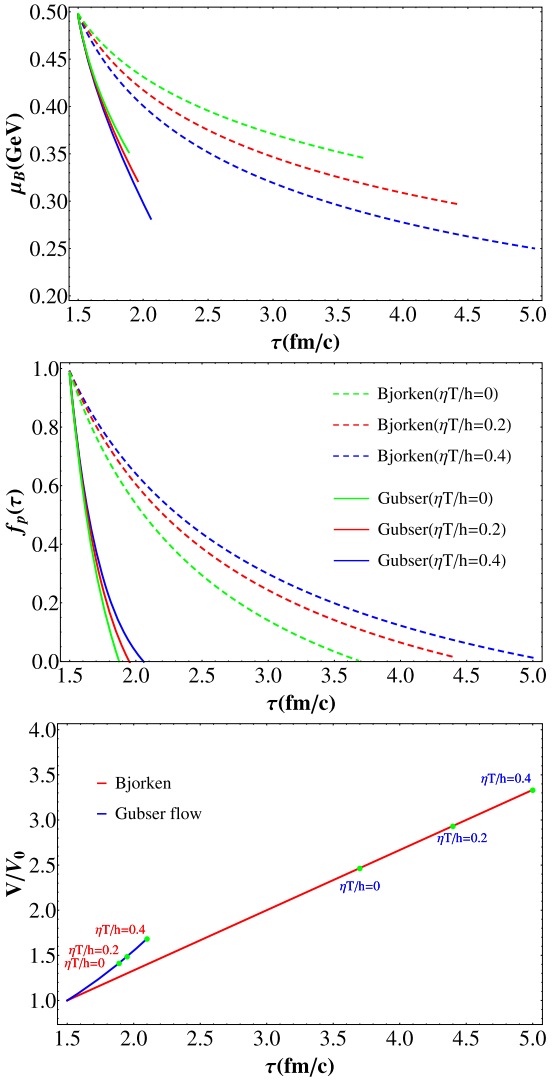

Fig. 3. Time evolution of μ_B, f_p, and volume increase for ideal and viscous hydrodynamic expansion. We set $\tau_c = 1.5$ fm/c and $\mu_B(\tau_c) = 0.5$ GeV.

expansion. As an example, the starting time of the phase transition τ_c was set to be 1.5 fm/c and μ_B at τ_c has been chosen to be 0.5 GeV. With these settings we obtain $n_{Bp} = 0.1948/\text{fm}^3$ and $s_p/n_{Bp} = 20$ at τ_c.

First we see that the results agree with the qualitative analyses done before. Compared with those with zero viscosities, the results with increasing viscosities show that the decrease of μ_B becomes stronger, the phase transition takes longer, and thus μ_B ends up with smaller final values, when the phase transition in the considered volume is complete. Second, the final value of μ_B in ideal hydrodynamic expansion does not depend on the expansion geometry, because both the entropy and net baryon number are conserved. In viscous expansion the entropy production depends on the expansion geometry. Therefore, the final value of μ_B in the Bjorken expansion is different from that in the Gubser expansion. Third, compared to the Bjorken expansion, the transverse expansion in the Gubser expansion leads to a stronger decrease of μ_B and faster phase transition.

In addition, we show in the last panel of Fig. 3 the volume increase during the phase transition, $V(\tau)/V(\tau_c)$. The points mark the volume increase at different end times of the phase transition. The rate of the volume increase is stronger in three-dimensional Gubser expansion than in one-dimensional Bjorken expansion. However, since the phase transition proceeds faster in Gubser expansion than in Bjorken expansion, the volume increase at the end of the phase transition is stronger in Bjorken expansion than in Gubser expansion.

The trajectory of s_m/n_{Bm} during the first-order phase transition is plotted in Fig. 2 for an ideal expansion (dashed straight line) and a viscous Bjorken expansion with $\eta_p T/h_p = 0.2$ (dotted curve).

Our results of the viscous effects on the dynamical evolution of QCD matter during the first-order phase transition could be refined, if more reliable EoS and transport coefficients of the parton and hadron phase were available and more realistic hydrodynamic expansion of QCD matter had been calculated at large baryon chemical potential. The present study is the basis for a further development of the dynamic transport simulation of the QCD phase transition in heavy-ion collisions [43].

4. Further discussions

In this section we discuss (or speculate) how the first-order phase transition will proceed with much larger viscosities, with which calculations using the first-order hydrodynamics may be invalid.

Recalling Eq. (16) at the starting time of the phase transition τ_c, where $f_p = 1$, we have

$$\frac{\partial e_m}{\partial \tau} = (e_p - e_h)\frac{df_p}{d\tau} + \frac{de_p}{d\mu_B}\frac{\partial \mu_B}{\partial \tau}. \tag{44}$$

For an expanding system $\partial e_m/\partial\tau$ is always negative, while its absolute value depends on the form of the expansion (U^μ) and viscosity. The larger the viscosity, the smaller is $|\partial e_m/\partial\tau|$. If the second term on the right hand side of Eq. (44), $(de_p/d\mu_B)(\partial\mu_B/\partial\tau)$, is positive, $df_p/d\tau$ should be negative, which indicates that the first-order phase transition will always proceed with any large viscosity, unless the viscous hydrodynamics breaks down. On the other hand, if $(de_p/d\mu_B)(\partial\mu_B/\partial\tau)$ is negative, $df_p/d\tau$ could be (mathematically) positive for sufficient large viscosity and slow expansion. A positive $df_p/d\tau$ at τ_c is not physical, which indicates that large viscosity may forbid the occurrence of first-order phase transition.

Both the signs of $de_p/d\mu_B$ and $\partial\mu_B/\partial\tau$ are determined by the EoS of the parton and hadron phase. For the EoS used in this work, both $de_p/d\mu_B$ and $\partial\mu_B/\partial\tau$ are negative. Thus, $df_p/d\tau$ at τ_c is always negative.

We have to note that for large viscosity the friction heat will be so large, that $\partial e_m/\partial\tau$ becomes positive when using the first-order hydrodynamics [see Eqs. (32), (33), and (17)]. A positive $\partial e_m/\partial\tau$ can lead to a positive $df_p/d\tau$ at τ_c according to Eq. (44). However, positive $\partial e_m/\partial\tau$ is impossible for an expanding system. In this case the first-order hydrodynamics is invalid and higher order terms have to be included in the hydrodynamic description of the phase transition.

The phase transition for $\tau > \tau_c$ seems more complicated. It cannot be proven from Eq. (16) that $df_p/d\tau$ is always negative with the used EoS, because $de_h/d\mu_B$ is positive. Thus, with sufficient large viscosity and slow expansion (slower than Bjorken and Gubser expansion), $df_p/d\tau$ may become positive and a transition of the net baryon number from the hadron phase to the parton phase may happen. However, this will not lead to the disappearance of the hadron phase, since $df_p/d\tau$ will be negative again at least at $f_p = 1$, as proven before. Thus, we expect that for large viscosity and slow expansion, the time evolution of f_p trends to decrease from 1 to 0, but maybe has some humps in between.

We note that at μ_B being smaller than the value at the critical point, the QCD phase transition is a crossover. Our formalism

developed in the previous section does not work in the crossover region. Although the exact position of the critical point connecting the crossover and first-order phase transition line is not known yet [3,4,7,8], various theoretical calculations suggest that its most probable location is in the μ_B interval between 200 and 400 MeV [44,45]. For large viscosity, the moving (μ_B, T) point along the first-order phase transition line may pass the critical point. Then critical phenomena are expected to occur.

The whole derivations in the previous section from Eq. (14) to Eq. (39) are also valid for the first-order phase transition in a contracting medium, where $dV/d\tau$ is negative. In this case, μ_B increases with time along the first-order phase transition line. We then describe a transition from the hadron phase to the parton phase.

In heavy-ion collisions the produced QCD matter expands on the whole. But locally on a small spatial scale, expansion as well as contraction exist due to density fluctuations. Our study provides a potential hydrodynamic framework to describe the nucleation of partons.

Acknowledgements

The authors are grateful to U. Heinz for reading the manuscript and very valuable comments. Z.X. thanks P. Huovinen, Y. Liu, N. Xu, and P. Zhuang for helpful discussions. This work was financially supported by the National Natural Science Foundation of China under Grants No. 11575092, No. 11335005, and No. 11275103, and the Major State Basic Research Development Program in China under Grants No. 2015CB856903. C.G. acknowledges support by the Deutsche Forschungsgemeinschaft (DFG) through the grant CRC-TR 211 “Strong-interaction matter under extreme conditions”.

References

[1] B. Mohanty, Nucl. Phys. A 830 (2009) 899C.
[2] F.R. Brown, F.P. Butler, H. Chen, N.H. Christ, Z.h. Dong, W. Schaffer, L.I. Unger, A. Vaccarino, Phys. Rev. Lett. 65 (1990) 2491.
[3] M. Asakawa, K. Yazaki, Nucl. Phys. A 504 (1989) 668.
[4] M.A. Stephanov, Prog. Theor. Phys. Suppl. 153 (2004) 139; Int. J. Mod. Phys. A 20 (2005) 4387.
[5] M.M. Aggarwal, et al., STAR Collaboration, Phys. Rev. Lett. 105 (2010) 022302.
[6] M.M. Aggarwal, et al., STAR Collaboration, arXiv:1007.2613 [nucl-ex].
[7] L. Kumar, STAR Collaboration, Nucl. Phys. A 904–905 (2013) 256c.
[8] X. Luo, Nucl. Phys. A 956 (2016) 75.
[9] P. Romatschke, U. Romatschke, Phys. Rev. Lett. 99 (2007) 172301.
[10] Z. Xu, C. Greiner, H. Stocker, Phys. Rev. Lett. 101 (2008) 082302; J. Uphoff, F. Senzel, O. Fochler, C. Wesp, Z. Xu, C. Greiner, Phys. Rev. Lett. 114 (11) (2015) 112301.
[11] H. Song, U.W. Heinz, J. Phys. G 36 (2009) 064033; C. Shen, S.A. Bass, T. Hirano, P. Huovinen, Z. Qiu, H. Song, U. Heinz, J. Phys. G 38 (2011) 124045.
[12] B.M. Waldhauser, D.H. Rischke, J.A. Maruhn, H. Stoecker, W. Greiner, Z. Phys. C 43 (1989) 411.
[13] E.V. Shuryak, Phys. Rep. 61 (1980) 71.
[14] C.P. Singh, P.K. Srivastava, S.K. Tiwari, Phys. Rev. D 80 (2009) 114508.
[15] H. Kouno, F. Takagi, Z. Phys. C 42 (1989) 209.
[16] C.P. Singh, B.K. Patra, S. Uddin, Phys. Rev. D 49 (1994) 4023.
[17] S.K. Tiwari, C.P. Singh, Adv. High Energy Phys. 2013 (2013) 805413.
[18] J. Cleymans, K. Redlich, H. Satz, E. Suhonen, Z. Phys. C 33 (1986) 151.
[19] D.H. Rischke, M.I. Gorenstein, H. Stoecker, W. Greiner, Z. Phys. C 51 (1991) 485.
[20] P. Braun-Munzinger, I. Heppe, J. Stachel, Phys. Lett. B 465 (1999) 15.
[21] K.A. Bugaev, M.I. Gorenstein, Z. Phys. C 43 (1989) 261.
[22] K.S. Lee, M.J. Rhoades-Brown, U.W. Heinz, Phys. Rev. C 37 (1988) 1452.
[23] L.P. Csernai, J.I. Kapusta, Phys. Rev. D 46 (1992) 1379.
[24] F. Gao, Y.x. Liu, Phys. Rev. D 94 (9) (2016) 094030.
[25] A. Muronga, Phys. Rev. C 69 (2004) 034903.
[26] E. Molnar, H. Niemi, D.H. Rischke, Eur. Phys. J. C 65 (2010) 615.
[27] C. Eckart, Phys. Rev. 58 (1940) 919.
[28] G.S. Denicol, S. Jeon, C. Gale, Phys. Rev. C 90 (2) (2014) 024912.
[29] J.D. Bjorken, Phys. Rev. D 27 (1983) 140.
[30] S.S. Gubser, Phys. Rev. D 82 (2010) 085027.
[31] S.S. Gubser, A. Yarom, Nucl. Phys. B 846 (2011) 469.
[32] J. Liao, V. Koch, Phys. Rev. C 80 (2009) 034904.
[33] P.F. Kolb, R. Rapp, Phys. Rev. C 67 (2003) 044903.
[34] N. Demir, S.A. Bass, Phys. Rev. Lett. 102 (2009) 172302.
[35] C. Sasaki, K. Redlich, Phys. Rev. C 79 (2009) 055207; Nucl. Phys. A 832 (2010) 62.
[36] A.S. Khvorostukhin, V.D. Toneev, D.N. Voskresensky, Nucl. Phys. A 845 (2010) 106.
[37] C. Wesp, A. El, F. Reining, Z. Xu, I. Bouras, C. Greiner, Phys. Rev. C 84 (2011) 054911.
[38] J. Noronha-Hostler, J. Noronha, C. Greiner, Phys. Rev. C 86 (2012) 024913.
[39] V. Ozvenchuk, O. Linnyk, M.I. Gorenstein, E.L. Bratkovskaya, W. Cassing, Phys. Rev. C 87 (6) (2013) 064903.
[40] S. Ryu, J.F. Paquet, C. Shen, G. Denicol, B. Schenke, S. Jeon, C. Gale, arXiv:1704.04216 [nucl-th].
[41] J. Auvinen, I. Karpenko, J.E. Bernhard, S.A. Bass, arXiv:1706.03666 [hep-ph].
[42] J. Liao, V. Koch, Phys. Rev. C 81 (2010) 014902.
[43] B. Feng, Z. Xu, C. Greiner, Phys. Rev. C 95 (2) (2017) 024907.
[44] Z. Fodor, S.D. Katz, J. High Energy Phys. 0404 (2004) 050.
[45] R.V. Gavai, S. Gupta, Phys. Rev. D 71 (2005) 114014.